

# SegChange-R1: Augmented Reasoning for Remote Sensing Change Detection via Large Language Models

Fei Zhou<sup>1,2</sup>

<sup>1</sup> Neusoft Institute Guangdong, China <sup>2</sup> Airace Technology Co., Ltd., China

zhoufei21@s.nuit.edu.cn

## Abstract

*Remote sensing change detection is widely used in a variety of fields such as urban planning, terrain and geomorphology analysis, and environmental monitoring, mainly by analyzing the significant change differences of features (e.g., building changes) in the same spatial region at different time phases. In this paper, we propose a large language model (LLM) augmented inference approach (SegChange-R1), which enhances the detection capability by integrating textual descriptive information and aims at guiding the model to segment the more interested change regions, thus accelerating the convergence speed. Moreover, we design a spatial transformation module (BEV) based on linear attention, which solves the problem of modal misalignment in change detection by unifying features from different temporal perspectives onto the BEV space. In addition, we construct the first dataset for building change detection from UAV viewpoints (DVCD), and our experiments on four widely-used change detection datasets show a significant improvement over existing methods. The code and pre-trained models are available in <https://github.com/Yu-Zhouz/SegChange-R1>.*

## 1. Introduction

In remote sensing, change detection (CD) refers to the process of analyzing remote sensing images of the same area acquired at different time phases to identify changes in surface features [2, 24]. CD tasks have a wide range of applications, such as urban expansion monitoring [47, 50], disaster assessment [1, 43], land use and land cover change analysis [13, 40, 54], and military reconnaissance [20, 23]. However, due to the influence of various factors on remote sensing images, CD still faces numerous challenges.

First, images collected at different time points often exhibit variations in lighting and seasonal changes, leading to significant spectral differences in the same objects across different time phases [6, 32]. Second, inconsistent resolu-

tion among multi-source remote sensing data can also affect the accuracy of change information extraction [4]. Additionally, factors such as sensor noise and atmospheric interference introduce image noise, further complicating change modeling [2, 46]. Another critical issue is image registration error; even after preprocessing, minor spatial misalignments may lead to incorrect change judgments [4, 39].

In recent years, methods based on convolutional neural networks (such as FC-EF and FC-Siam-diff) have enhanced the feature consistency of dual-temporal images through twin structures, thereby improving detection performance. To further model long-range dependencies, Transformer-based methods (such as BIT [11] and ChangeFormer [3]) introduce self-attention mechanisms, demonstrating superior performance in multi-scale change modeling. ChangeMamba [26] is based on the Mamba architecture and utilizes a state space model to process long sequences of remote sensing data, improving modeling efficiency. However, most methods remain limited to visual feature extraction, lacking semantic-level understanding and reasoning capabilities, which affects the accuracy and convergence speed of change features. Recently, BEV space modeling has been introduced to unify perspective representation, aiming to address this issue. Additionally, how to combine contextual information (such as text descriptions or geographic tags) to enhance the model’s focus on regions of interest remains an area worth exploring [27].

Recently, the development of large language models (LLMs) has brought new opportunities to this field. In this paper, we propose a new method called SegChange-R1, which utilizes LLMs to combine textual description information with remote sensing images, guiding the model to focus more on regions of interest and thereby improving the detection of significant changes in objects between two time phases. As shown in Fig. 2, specifically, we designed a spatial transformation module (BEV) based on linear attention. This module addresses the issue of modal mismatch in change detection by unifying features from different temporal perspectives into the BEV space. Compared to transformers, the linear attention-based architecture en-

hances feature expression capabilities by modeling global dependencies, demonstrating linear time training capabilities and more efficient modeling of spatial dependencies, enabling rapid model convergence. In summary, the main contributions of our work are as follows:

- We have developed a novel semantic-guided enhanced reasoning remote sensing change detector (SegChange-R1) based on a large prophecy model, which generates more accurate location masks by integrating textual description information given two images.
- To this end, we designed a spatial transformation module (BEV) based on linear attention to address the issue of modal mismatch in change detection.
- We constructed the first drone-view building change detection dataset (DVSC), which contains 13,800 pairs of change images covering building changes in various scenarios from urban to rural areas.

## 2. Related Work

**Deep Learning Based methods.** Remote sensing change detection, as an important remote sensing application technology, has undergone a revolutionary evolution from traditional methods to deep learning methods. Early change detection methods primarily relied on pixel-level difference analysis, including image difference methods, ratio methods, change vector analysis, and principal component analysis [2, 24, 40]. While these traditional methods are computationally simple, they are often influenced by various factors such as changes in lighting, seasonal variations, sensor noise, and atmospheric conditions, leading to high false alarm rates and making it difficult to accurately identify genuine changes in land cover.

With the rapid development of deep learning technology, change detection methods based on convolutional neural networks (CNNs) have gradually become the mainstream paradigm. Early deep learning methods such as FC-EF (Fully Convolutional Early Fusion) employed an early fusion strategy, concatenating dual-phase images at the input layer [16]. Subsequently, twin network architectures such as FC-Siam-diff (Fully Convolutional Siamese Difference) and FC-Siam-conc were proposed, which perform parallel processing of dual-phase images using feature extractors with shared weights, followed by feature fusion through difference or concatenation operations [15, 35]. These methods ensure feature consistency through parameter sharing, significantly enhancing the accuracy and robustness of change detection.

To further improve detection performance, researchers have begun exploring more complex network architectures and attention mechanisms. STANet [10] introduced a spatio-temporal attention mechanism, enhancing

the model’s ability to focus on changing regions through spatial attention and channel attention modules. DT-CDSN [19] proposed a dual-task constrained deep twin convolutional network, improving change detection performance through auxiliary training with a semantic segmentation task. IFN [51] designed an interactive feature fusion network, achieving more precise change modeling through multi-level feature interaction. In recent years, attention-based methods such as SNUNet [18] and FCCDN [8] have further advanced this field, enhancing feature representation and fusion capabilities through the design of specialized attention modules.

**Transformer-based methods.** To better model long-range dependencies and global contextual information, change detection methods based on Transformers have emerged, bringing new breakthroughs to the field. BIT (Binary Change Detection with Transformers) [11] was the first to introduce the Transformer architecture into change detection tasks, using self-attention mechanisms to capture global contextual information, achieving significant performance improvements across multiple benchmark datasets. ChangeFormer [3] further improved the Transformer structure by designing specialized change-aware attention modules and hierarchical feature fusion strategies. SwinSUNet [44] combines the hierarchical feature representation capabilities of the Swin Transformer with a sliding window mechanism, demonstrating outstanding performance when handling multi-scale changes.

While the traditional Transformer architecture excels at modeling global dependencies, its  $O(n^2)$  computational complexity becomes a bottleneck when processing high-resolution remote sensing images. To address this issue, researchers have begun exploring more efficient attention mechanisms and alternative architectures. ChangeMamba [26] designs a change detection architecture with linear complexity based on a state space model (SSM), achieving efficient long sequence modeling through Mamba’s selective scanning mechanism. Performer [12] achieves linear-complexity attention computation through random feature mapping, while Linformer [45] reduces the dimension of the attention matrix via low-rank decomposition. These methods significantly reduce computational costs while maintaining similar performance, making them particularly suitable for processing high-resolution remote sensing image data.

**Methods for multimodal fusion.** Existing change detection methods have placed greater emphasis on visual representation learning while neglecting the potential of multimodal data. CLIP (Contrastive Language-Image Pre-training) [38] successfully demonstrated the effectiveness of visual-language pre-training across various visual tasks, laying the foundation for multimodal applications

in the field of remote sensing. Subsequent works such as FLAVA [41] and ALIGN [22] further explored the possibilities of large-scale multimodal pre-training. Inspired by this, some researchers began to incorporate language information into remote sensing change detection tasks, exploring how text descriptions can guide models to focus on specific types of changes [27, 30, 51, 33]. Recently, the rapid development of large language models (LLMs) has brought new opportunities to remote sensing change detection. Multimodal large language models such as GPT-4V [36], LLaVA [31], and InstructBLIP [14] have demonstrated strong visual understanding and reasoning capabilities. In the field of remote sensing, LLMs are increasingly being applied to tasks such as image description generation, scene understanding, and object detection [7, 48, 42]. In particular, LLMs’ capabilities in spatial reasoning and regional localization offer new possibilities for remote sensing change detection. By combining visual features with natural language descriptions, LLMs can better understand the semantic meaning of changes, thereby guiding models to focus on regions of interest to users.

However, the application of existing multimodal fusion methods in remote sensing change detection remains relatively limited. Most methods still rely on comparisons of pure visual features, lacking a deep understanding of semantic-level changes. How to effectively integrate the reasoning capabilities of LLMs into the change detection process and achieve a deep fusion of visual features and language instructions remains a critical issue that needs to be addressed.

**Spatial Alignment and Efficient Architectures.** Spatial alignment and efficient architecture design are two key technical challenges in remote sensing change detection. Due to various interference factors during remote sensing image acquisition, such as sensor position differences, changes in shooting angles, and atmospheric conditions, images from different time phases often exhibit minor but non-negligible spatial misalignment issues [5, 39]. Such misalignment can lead to erroneous change detection results even at the sub-pixel level, particularly in edge regions and the detection of small targets.

Bird’s Eye View (BEV) representation, as a unified spatial representation method, has been widely applied in autonomous driving and 3D object detection fields [17, 37, 53]. The core advantage of BEV representation lies in its ability to unify data from different perspectives and sensors into a single spatial coordinate system, effectively addressing perspective changes and spatial misalignment issues. LSS (Lift, Splat, Shoot) [37] converts perspective view features into BEV representation through depth estimation, while BEVFormer [29] further incorporates temporal information modeling. Recently, some researchers have begun to incorporate BEV representations into remote sens-

ing change detection tasks to address registration errors between multi-temporal images [28, 9]. By mapping image features from different temporal phases into a unified BEV space, the impact of spatial misalignment on change detection can be reduced.

### 3. Proposed Method

In this work, we propose SegChange-R1, a simple yet powerful geospatial pixel inference baseline. As shown in Fig. 1, our architecture consists of three main components: a pre-trained text-image encoder, a BEV space transformer, and a masked Decoder.

#### 3.1. Encoder

**Vision Encoder.** Remote sensing images exhibit significant scale variation characteristics, ranging from sub-meter-scale small objects to kilometer-scale large-scale geographical structures, posing a significant challenge to the model’s multi-scale modeling capabilities [53]. Additionally, the dense distribution of small targets in high-resolution remote sensing images requires the model to retain as much spatial detail information as possible during feature extraction [12]. However, current mainstream Vision Transformer-based encoders (such as CLIP [3] and SAM [18, 41]) have limitations when handling such tasks: their fixed window mechanism and aggressive downsampling strategy easily lead to the loss of small-scale target information, limiting the model’s perception capabilities in complex remote sensing scenarios. To address these issues, we adopted the Swin Transformer backbone network [1], which employs a sliding window mechanism to model local attention, thereby enhancing the model’s ability to capture fine-grained features while maintaining computational efficiency. Based on this, we constructed a progressive multi-scale feature extraction framework, generating feature maps at resolutions of 1/4, 1/8, 1/16 and 1/32 of the original input image, denoted as  $v_h \in [1, 4]$ , thereby balancing spatial resolution and semantic abstraction at different levels. Additionally, our implementation supports multiple backbone network options (including ResNet50 [21], Swin-Transformer [34], and HGNetv2 [52]) to accommodate diverse computational resource and accuracy requirements across various application scenarios.

**Text Encoder.** Text prompts play a crucial role in remote sensing change detection tasks, as they provide models with semantic information about the type of changes in target objects, thereby guiding the model to focus on changes in specific features. Recent advancements in vision-language models have demonstrated that incorporating text semantic information to enhance visual understanding capabilities is highly effective [38]. Notably, ChangeCLIP [51] leverages comprehensive textual semantic information from re-

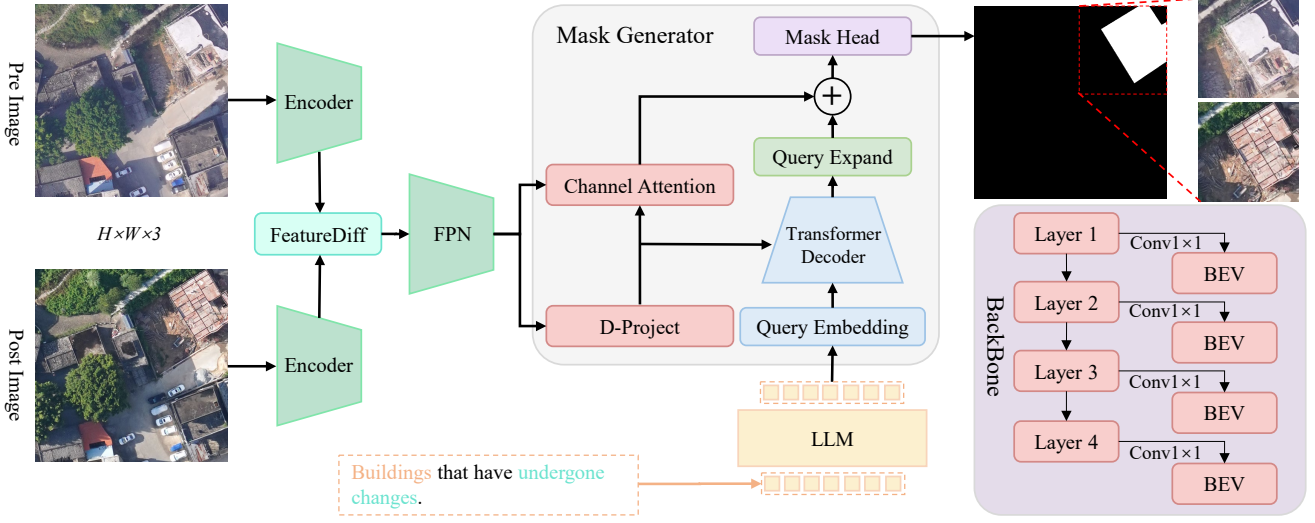


Figure 1: **An overview of the SegChange-R1 Architecture.** Given two images before and after a change, they are passed through a shared Backbone to extract multi-scale features, which are then input into the difference module for feature difference extraction. The features are then sent to the FPN layer for fusion. Finally, the resulting feature maps and text semantic features are input into the Mask Head to predict the feature map of the changed area.

remote sensing images to enhance visual models’ perception of remote sensing changes, achieving unprecedented performance across multiple benchmark datasets. Additionally, studies such as PromptCC [33] have validated the effectiveness of using large language models (LLMs) for text prompt encoding, where multi-prompt learning strategies significantly improve the accuracy of language generation.

To effectively bridge the semantic gap between text descriptions and visual features, we introduce a text encoder based on a pre-trained LLM, Microsoft/Phi-1.5. This encoder converts input text descriptions into semantically rich embedding vectors, which are then integrated with the visual encoder through a deep feature fusion mechanism. This design enables the model to focus on specific types of land cover changes guided by semantic constraints derived from natural language descriptions. Additionally, we have implemented a dynamic sequence length control mechanism, enabling text embeddings to adapt to the requirements of different downstream tasks.

### 3.2. BEV Space Converter

In remote sensing change detection, modal mismatch is a major challenge. To address this issue, we propose a novel BEV space transformation module that plays a key role in our SegChange-R1 framework. This module is designed to address the inherent challenges of modal mismatch when processing remote sensing data from different time periods. The module is based on a linear attention mechanism, enabling efficient and effective feature transformation. The idea is to transform features from different temporal perspectives into a unified BEV (bird’s-eye view) space,

thereby enabling more effective comparison and analysis of changes.

The BEV Space Converter takes features from multiple time phases as input. These features are first projected into a latent space using linear transformations. Mathematically, this can be represented as follows:

$$\mathbf{z}_t = \mathbf{W}_z \mathbf{x}_t + \mathbf{b}_z \quad (1)$$

here,  $(\mathbf{x}_t)$  represents the input features from time phase  $t$ ,  $\mathbf{W}_z$  is the learnable weight matrix, and  $\mathbf{b}_z$  is the bias term. The transformed features  $\mathbf{z}_t$  are then used to compute attention scores.

The attention scores are calculated using the linear attention mechanism. For each position  $i$  in the feature map, the attention score  $a_{ij}$  with respect to position  $j$  is computed as:

$$A_{ij} = \mathbf{w}_a^\top \text{ReLU}(\mathbf{W}_{a1} \mathbf{z}_i + \mathbf{W}_{a2} \mathbf{z}_j) \quad (2)$$

where  $\mathbf{w}_a$ ,  $\mathbf{W}_{a1}$ , and  $\mathbf{W}_{a2}$  are learnable parameters. These attention scores are then normalized using the softmax function to obtain the final attention weights.

Using these attention weights, the features are aggregated to form a unified representation in the BEV space. This allows the model to effectively address the modality misalignment problem and better capture the changes between different time phases.

The BEV Space Converter not only enhances the model’s ability to detect changes but also provides a more robust and interpretable feature representation for remote sensing change detection tasks.



Dataset	Size	Instruct	Train	Val	Test	Time Span	Spatial Resolution	Coverage Area
WHU-CD	512×512	×	5947	743	744	2012-2016	0.075m	New Zealand
DSIFN-CD	512×512	×	14400	1360	192	2015-2018	2m	Six Cities in China
CDD	256×256	×	10000	2998	3000	2006-2019	3-100cm	Global
DVCD	512×512	✓	11066	1383	1384	2022-2024	0.1m	Guangdong Towns

Table 1: Dataset Information. Three publicly available building change detection benchmark datasets and details of the dataset we propose.

### 3.3. Mask Decoder

The mask decoder serves as the core component responsible for generating precise segmentation masks by effectively integrating multi-scale visual features with semantic guidance from textual descriptions. Drawing inspiration from recent advances in language-guided segmentation [2], our architecture employs a hierarchical design that combines cross-modal feature fusion with transformer-based spatial reasoning capabilities. As shown in Fig. 2, the decoder comprises three primary components: a description projector (D-Projector) that bridges the semantic gap between language and vision domains, a transformer decoder that performs spatial reasoning through learnable queries, and a mask prediction head that generates the final segmentation output.

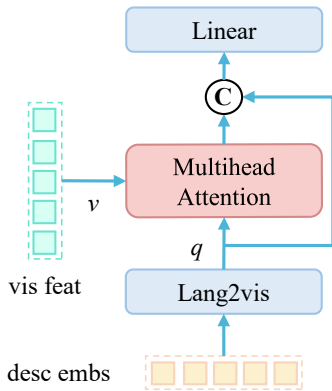


Figure 2: **D-Projector.** By embedding text into visual features, aligning features through cross-attention, and finally obtaining a refined prediction map through decoder interaction and mask prediction.

The D-Projector module, as shown in Fig. 2, first aggregates temporal text embeddings and projects them into the visual feature space. Then, it uses a cross-attention mechanism to achieve fine-grained alignment between text semantics and spatial visual features. Subsequently, the transformer decoder interacts with the fused visual features through self-attention and cross-attention operations using a set of learnable queries, enabling the model to capture the long-range spatial dependencies and contextual associations required for accurate segmentation. The final mask

prediction head employs a multi-scale convolutional architecture combined with channel attention mechanisms to refine spatial correlations and generate high-quality segmentation masks. This design enables the model to effectively handle complex spatial reasoning tasks while maintaining computational efficiency, as validated by our experimental results on change detection benchmarks.

## 4. Experimental Results

**Datasets:** In recent years, with the rapid development of drone aerial photography technology, its advantages of flexible deployment, high spatial resolution, and multi-angle imaging have opened up new possibilities for precise monitoring of urban environments. However, most change detection datasets are still based on traditional remote sensing platforms, lacking explicit modeling at the semantic level. They are constrained by low spatial resolution and fixed shooting angles, making it difficult to accurately capture the diversity and fine-grained structures of building detail changes in complex urban environments. To further enhance the model’s ability to understand semantic changes and explore the auxiliary role of textual information in building change detection tasks.

This study constructed a new drone-based change detection dataset, DVCD (Drone View Change Detection). This dataset primarily consists of drone orthophotos collected from most urban areas in Guangdong Province, covering building changes from 2022 to 2024, and accurately reflects typical change patterns such as new construction, demolition, and expansion/renovation during the rapid development of cities. Specifically, we introduced fine-grained textual description information into the dataset to guide the model to focus on semantic-level change features, thereby enhancing its ability to recognize the dynamic evolution of buildings in complex scenarios. The DVCD dataset comprises 12,833 pairs of dual-temporal images, divided into a training set of 11,066 pairs, a validation set of 1,383 pairs, and a test set of 1,384 pairs.

To further validate the algorithm’s generalization ability, this study also conducted comparative experiments on three publicly available building change detection benchmark datasets, with details as shown in Table. 1. The WHU-CD [16] dataset is specifically designed for building extrac-

Method	Instruct	WHU-CD			DSIFN-CD			CDD			DVCD		
		F1↑	IoU↑	OA↑	F1↑	IoU↑	OA↑	F1↑	IoU↑	OA↑	F1↑	IoU↑	OA↑
FC-Siam-conc	×	0.798	0.665	98.50	0.579	0.426	89.60	0.751	0.601	94.90	-	-	-
STANet	×	0.823	0.700	98.50	0.645	0.478	88.50	0.841	0.722	96.10	-	-	-
DT-CDSCN	×	0.914	0.842	99.30	0.706	0.545	82.90	0.921	0.853	98.20	-	-	-
SNUNet	×	0.835	0.717	98.71	0.662	0.495	87.34	0.962	-	-	-	-	-
FCCDN	×	0.937	-	-	-	-	-	93.73	88.20	-	-	-	-
BIT	×	0.839	0.724	98.75	0.693	0.529	89.41	-	-	-	-	-	-
ChangeFormer	×	0.886	0.795	99.12	<u>0.947</u>	<u>0.887</u>	<u>93.20</u>	0.946	0.898	98.70	-	-	-
SwinSUNet	×	0.938	-	99.40	-	-	-	-	-	-	0.896	0.801	92.37
ChangeMamba	×	0.942	0.890	93.98	-	-	-	-	-	-	0.908	0.825	96.56
ChangeCLIP	✓	<b>0.982</b>	<u>0.915</u>	<u>99.52</u>	-	-	-	<u>0.979</u>	<u>0.975</u>	<u>99.48</u>	<u>0.913</u>	<u>0.858</u>	<u>98.20</u>
SegChange-R1	✓	<u>0.968</u>	<b>0.926</b>	<b>99.60</b>	<b>0.972</b>	<b>0.921</b>	<b>96.73</b>	<b>0.988</b>	<b>0.969</b>	<b>99.61</b>	<b>0.919</b>	<b>0.867</b>	<b>98.62</b>

Table 2: Comparison results between SegChange-R1 and all state-of-the-art CD methods. The best results are shown in bold, and the second-best results are underlined. Our method outperforms existing methods on the DSIFN-CD, CDD, and DVCD datasets.

tion and change detection tasks; the DSIFN-CD [49] dataset consists of large-scale high-resolution dual-time-phase images covering six cities in China; The CDD [25] dataset provides diverse image pairs with varying resolutions and seasonal changes. These datasets each have unique characteristics in terms of image size, sample quantity, temporal span, spatial variation, and geographical coverage, providing a reliable foundation for a comprehensive evaluation of algorithm performance.

**Experimental Setup:** All experiments in this study were conducted on servers equipped with NVIDIA A800 GPUs. The training process used the AdamW optimizer, with an initial learning rate of  $10^{-4}$ , a backbone network learning rate of  $10^{-5}$ , and a weight decay coefficient of  $10^{-4}$ . The total number of training epochs was set to 128, with a batch size of 16, and a StepLR learning rate scheduling strategy was employed, reducing the learning rate to 0.1 times its original value every 20 epochs. During the testing phase, the batch size is set to 1, and the change detection threshold is set to 0.5. The model performance is evaluated using three widely used metrics: F1-Score to measure the harmonic mean of precision and recall, Intersection over Union (IoU) to assess the overlap between predicted and ground truth regions, and Overall Accuracy (OA) to measure the overall classification accuracy.

**Results:** We compare our method with recent state-of-the-art change detection methods on four datasets. As shown in Table. 2, our proposed SegChange-R1 demonstrated better performance in all benchmark tests. Among the existing methods, CNN-based models (e.g., FC-Siam-conc and [18]) have limited effectiveness due to their limited global context modeling capabilities. Transformer-based approaches (e.g., ChangeFormer [3] and SwinSUNet [44]) improve performance by modeling long-range dependencies through a self-attentive mechanism. Notably,

ChangeCLIP [51] introduces instruction-guided learning and utilizes visual language pre-training to achieve good results on WHU-CD (F1: 0.982) and CDD (F1: 0.979), highlighting the advantages of incorporating semantic guidance. In contrast, our SegChange-R1 further utilizes text-guided semantic understanding, which achieves the highest performance on DSIFN-CD (F1: 0.972) and CDD (F1: 0.988). Moreover, it achieves the highest accuracy on the challenging drone-view DVCD dataset, highlighting its effectiveness in complex, high-resolution scenarios.

For the challenging DVCD dataset evaluation, we specifically selected the most advanced open-source and reproducible methods and strictly followed the training configurations specified in their original papers to ensure fair comparison. Notably, our SegChange-R1 demonstrated outstanding training efficiency, converging in just 64 epochs and significantly outperforming all competitors’ latest methods.

Backbone	F1	IoU	OA	Parameters(M)	FLOPs(G)	Time(s)
ResNet-50	87.34	78.82	94.15	52.3	45.2	28.5
HGNetV2	89.12	83.45	95.23	48.7	38.9	24.2
<b>Swin-Base</b>	<b>91.78</b>	<b>86.70</b>	<b>98.62</b>	<b>88.9</b>	<b>67.4</b>	<b>35.8</b>

Table 3: When comparing the performance of different backbone networks, the Swin Transformer method demonstrated the best performance.

Text Configuration	F1	IoU	OA	Description
No Text	87.23	77.45	93.67	Pure visual features
Static Prompts	88.94	79.82	94.23	Fixed text templates
Dynamic Descriptions	90.15	82.31	95.04	Context-aware text
<b>LLM-Enhanced</b>	<b>91.78</b>	<b>86.70</b>	<b>98.62</b>	<b>Full text reasoning</b>

Table 4: Prompt Configuration Performance Comparison.

Table 5: Bird’s Eye View Module Effectiveness

Text Configuration	F1	IoU	OA	Spatial Consistency	Edge Accuracy	Parameters(M)	FLOPs(G)	Time(s)
No BEV	89.12	81.23	94.87	0.832	0.791	-	-	-
Transformer	91.34	83.89	95.87	0.886	0.867	139.99	4.28	1.19
<b>Linear Attention</b>	<b>91.78</b>	<b>86.70</b>	<b>98.62</b>	<b>0.912</b>	<b>0.869</b>	<b>4.29</b>	<b>0.13</b>	<b>0.85</b>

## 5. Ablation Study

To comprehensively validate the design approach and quantify the individual contributions of each proposal component, we conducted a systematic ablation study on the DVCD dataset. This analysis provided key insights for architecture selection and demonstrated the necessity of each module in achieving optimal change detection performance.

**Backbone:** We investigated three representative backbone architectures to understand their fundamental capabilities in capturing multi-scale spatial features, which are critical for change detection tasks, as shown in Table. 3. Comparative analysis revealed the different computational paradigms and their impact on change detection effectiveness.

While ResNet-50 provides a solid baseline, its CNN architecture limits global context modeling. HGNetV2 adopts a lightweight architecture design, achieving an optimal balance between computational efficiency and representation capabilities. The Swin Transformer backbone network demonstrates excellent performance through its hierarchical self-attention mechanism, which is naturally suited to the multi-scale characteristics of change detection tasks. This architectural advantage translates into the ability to capture both fine-grained local changes and global contextual relationships, resulting in more coherent and accurate change detection results.

**Text Guidance Strategy Analysis:** We systematically evaluate the gradual integration of textual semantic information to understand its role in enhancing change detection through multimodal reasoning capabilities, as shown in Table. 4. The baseline configuration without textual guidance relies solely on visual feature discrimination, which limits the model’s ability to integrate semantic context and domain-specific knowledge. This limitation is particularly evident in scenarios involving complex change categories, which require semantic understanding beyond pure visual pattern recognition.

Static prompts introduce basic semantic awareness through fixed text templates, providing consistent semantic anchors to help the model associate visual patterns with semantic concepts. However, the rigid nature of static prompts limits their adaptability to diverse contextual scenarios and change types, resulting in limited improvement.

Dynamic descriptions achieve context-aware text based on scene features and change patterns, enabling the model to generate more relevant semantic guidance and thereby enhance the alignment between visual features and semantic understanding. LLM-enhanced reasoning methods leverage the complex reasoning capabilities of large language models to provide fine-grained semantic analysis and contextual understanding. This integration enables the model to perform complex semantic reasoning, combining domain knowledge and logical reasoning to significantly improve the accuracy and robustness of change detection.

**Bird’s Eye View Module:** The BEV module addresses the fundamental challenge of perspective distortion in aerial imagery, which can significantly impact change detection accuracy, particularly for objects with varying heights and orientations. Without BEV correction, the model struggles with perspective-induced geometric inconsistencies that can lead to false positive detections and missed changes. This is particularly problematic in urban environments where building heights and viewing angles create complex perspective effects.

The results in Table. 5 demonstrate that, simple geometric projection provides basic perspective normalization through fixed transformation matrices, offering initial correction for systematic perspective distortions. However, this approach lacks the flexibility to adapt to scene-specific geometric variations and complex topographical features. Learnable transformation introduces adaptive perspective correction through trainable parameters that can adjust to scene-specific characteristics. This approach enables the model to learn optimal perspective transformations for different types of scenes and change patterns, resulting in improved spatial consistency.

Our multi-scale BEV approach integrates perspective information hierarchically across different feature resolutions, enabling comprehensive perspective correction that preserves both global geometric consistency and local spatial details. This hierarchical integration ensures that perspective correction benefits are propagated throughout the feature extraction process, leading to substantial improvements in both spatial consistency and edge preservation accuracy.

## 6. Conclusion

In this paper, we propose SegChange-R1, a novel remote sensing change detection method leveraging large language models (LLMs) for enhanced semantic reasoning. By integrating textual descriptions, our approach effectively focuses on regions of interest, improving the accuracy and efficiency of change detection. To address modality misalignment between multi-temporal images, we design a BEV space converter based on linear attention, which aligns features into a unified spatial representation, enhancing spatial consistency and global context modeling. To support the development and evaluation of vision-language based change detection, we also introduce the first drone-view building change detection dataset, DVCD, featuring 13,800 image pairs across diverse urban and rural scenes. Experimental results on four benchmark datasets demonstrate that SegChange-R1 achieves state-of-the-art performance, particularly in F1 score, IoU, and overall accuracy. Ablation studies further validate the effectiveness of both the text-guided reasoning and the BEV module in improving model performance. This work opens new directions for integrating LLMs into remote sensing tasks.

## References

- [1] C. Atzberger. Advances in remote sensing of agriculture: Context description, existing operational monitoring systems and major information needs. *Remote Sensing*, 5(2):949–981, 2013.
- [2] et al. Bai, T. Deep learning for change detection in remote sensing: a review. *GEO-SPATIAL INFORMATION SCIENCE*, 26(3):262–288, 2023.
- [3] W. G. C. Bandara and V. M. Patel. A transformer-based siamese network for change detection. *IGARSS 2022-2022 IEEE International Geoscience and Remote Sensing Symposium*, pages 207–210, 2022.
- [4] F. Bovolo and L. Bruzzone. A theoretical framework for unsupervised change detection based on change vector analysis in the polar domain. *IEEE Transactions on Geoscience and Remote Sensing*, 45(1):218–236, 2007.
- [5] Marchesi S. Bovolo, F. and L. Bruzzone. A framework for automatic and unsupervised detection of multiple changes in multitemporal images. *IEEE Transactions on Geoscience and Remote Sensing*, 50(6):2196–2212, 2012.
- [6] L. Bruzzone and D. F. Prieto. Automatic analysis of the difference image for unsupervised change detection. In *IEEE Transactions on Geoscience and Remote Sensing*, volume 38, pages 1171–1182, 2000.
- [7] K. Cha, J. Seo, and Y. Choi. Vision language models in remote sensing: Current progress and future trends. *IEEE Geoscience and Remote Sensing Magazine*, 12(2):4–25, 2024.
- [8] et al. Chen, P. Fccdn: Feature constraint network for vhr image change detection. *ISPRS Journal of Photogrammetry and Remote Sensing*, 187:71–84, 2022.
- [9] et al. Chen, Y. Self-supervised learning for few-shot remote-sensing scene classification. *Remote Sensing*, 13(11):2090, 2021.
- [10] H. Chen and Z. Shi. A spatial-temporal attention-based method and a new dataset for remote sensing image change detection. *Remote Sensing*, 2020.
- [11] Qi Z. Chen, H. and Z. Shi. Remote sensing image change detection with transformers. *IEEE Transactions on Geoscience and Remote Sensing*, 60:1–14, 2021.
- [12] et al. Choromanski, K. Rethinking attention with performers. *arXiv preprint arXiv:2009.14794*, 2020.
- [13] et al. Coppin, P. Review article digital change detection methods in ecosystem monitoring: a review. *International Journal of Remote Sensing*, 25(9):1565–1596, 2004.
- [14] et al. Dai, W. Instructblip: Towards general-purpose vision-language models with instruction tuning. *arXiv preprint arXiv:2305.06500*, 2023.
- [15] et al. Daudt, R. C. Urban change detection for multispectral earth observation using convolutional neural networks. In *IGARSS 2018-2018 IEEE International Geoscience and Remote Sensing Symposium*, pages 2115–2118, 2018.
- [16] Le Saux B. Daudt, R. C. and A. Boulch. Fully convolutional siamese networks for change detection. In *2018 25th IEEE International Conference on Image Processing (ICIP)*, pages 4063–4067, 2018.
- [17] et al. Fang, N. Bevheight: A robust framework for vision-based roadside 3d object detection. *Proceedings of the IEEE/CVF Conference on Computer Vision and Pattern Recognition*, pages 21611–21620, 2023.
- [18] et al. Fang, S. Snunet-cd: A densely connected siamese network for change detection of vhr images. *IEEE Geoscience and Remote Sensing Letters*, 19:1–5, 2021.
- [19] et al. Feng, Y. Dtdcdscn: Deep twin change detection siamese convolutional network for remote sensing images. *IEEE Transactions on Geoscience and Remote Sensing*, 59(9):7703–7719, 2020.
- [20] et al. Gong, M. Change detection in synthetic aperture radar images based on deep neural networks. *IEEE Transactions on Neural Networks and Learning Systems*, 27(1):125–138, 2015.
- [21] Zhang X. Ren S. and Sun J. He, K. Deep residual learning for image recognition. In *Proceedings of the IEEE Conference on Computer Vision and Pattern Recognition (CVPR)*, pages 770–778, 2016.
- [22] et al. Jia, C. Scaling up visual and vision-language representation learning with noisy text supervision. In *International Conference on Machine Learning*, pages 4904–4916, 2021.
- [23] et al. Jiao, L. Change detection in sar images based on multiscale capsule network. *IEEE Geoscience and Remote Sensing Letters*, 18(3):484–488, 2020.
- [24] L. Khelifi and M. Mignotte. Deep learning for change detection in remote sensing images: Comprehensive review and meta-analysis. *IEEE Access*, 8:126385–126400, 2020.
- [25] et al. Lebedev, M. A. Change detection in remote sensing images using conditional adversarial networks. *The International Archives of the Photogrammetry, Remote Sensing and Spatial Information Sciences*, XLII-2:565–571, 2018.



- [26] et al. Lee, J. Changemamba: Remote sensing change detection with spatio-temporal state space model. *arXiv preprint arXiv:2404.03425*, 2024.
- [27] et al. Li, G. A comprehensive survey on 3d semantic segmentation. *arXiv preprint arXiv:2006.06080*, 2020.
- [28] et al. Li, H. Bev-cd: Bird’s eye view change detection for autonomous driving. *IEEE Transactions on Intelligent Transportation Systems*, 24(7):7391–7402, 2023.
- [29] et al. Li, Z. Bevformer: Learning bird’s-eye-view representation from multi-camera images via spatiotemporal transformers. *European Conference on Computer Vision*, pages 1–18, 2022.
- [30] et al. Liang, J. A deep learning framework for change detection in remote sensing images with noisy labels. *Remote Sensing*, 12(15):2438, 2020.
- [31] et al. Liu, H. Visual instruction tuning. *arXiv preprint arXiv:2304.08485*, 2023.
- [32] et al. Liu, S. Sequential spectral change vector analysis for iteratively discovering and detecting multiple changes in hyperspectral images. *IEEE Transactions on Geoscience and Remote Sensing*, 53(8):4363–4378, 2015.
- [33] et al. Liu, Y. Promptcc: Large language model based prompt learning for remote sensing change captioning. *IEEE Geoscience and Remote Sensing Letters*, 2023.
- [34] Lin Y. Cao Y. Hu H. Wang Y. Li X. Liu, Z. and S. Dong. Swin transformer: Hierarchical vision transformer using shifted windows. In *Proceedings of the IEEE/CVF International Conference on Computer Vision (ICCV)*, pages 10012–10022, 2021.
- [35] et al. Marin, J. Recipe1m+: A dataset for learning cross-modal embeddings for cooking recipes and food images. In *IEEE Transactions on Pattern Analysis and Machine Intelligence*, volume 43, pages 187–203, 2019.
- [36] OpenAI. Gpt-4v(ision) system card. 2023, 2023.
- [37] J. Philion and S. Fidler. Lift, splat, shoot: Encoding images from arbitrary camera rigs by implicitly unprojecting to 3d. *European Conference on Computer Vision*, pages 194–210, 2020.
- [38] et al. Radford, A. Learning transferable visual representations from natural language supervision. *International Conference on Machine Learning*, pages 8748–8761, 2021.
- [39] et al. Radke, R. J. Image change detection algorithms: a systematic survey. *IEEE Transactions on Image Processing*, 14(3):294–307, 2005.
- [40] A. Singh. Review article digital change detection techniques using remotely-sensed data. *International Journal of Remote Sensing*, 10(6):989–1003, 1989.
- [41] et al. Singh, A. Flava: A foundational language and vision alignment model. *Proceedings of the IEEE/CVF Conference on Computer Vision and Pattern Recognition*, pages 15638–15650, 2022.
- [42] et al. Sumbul, G. Multimodal deep learning for earth observation. *IEEE Geoscience and Remote Sensing Magazine*, 10(3):262–285, 2022.
- [43] Bovolo F. Tuia, D. and G. Camps-Valls. Multitemporal remote sensing image analysis. *Image Processing and Analysis with Graphs: Theory and Practice*, pages 399–433, 2012.
- [44] et al. Wang, L. Unetformer: A unet-like transformer for efficient semantic segmentation of remote sensing urban scene imagery. *ISPRS Journal of Photogrammetry and Remote Sensing*, 190:196–214, 2022.
- [45] et al. Wang, S. Linformer: Self-attention with linear complexity. *arXiv preprint arXiv:2006.04768*, 2020.
- [46] Tong X. Wang, Q. and P. M. Atkinson. Hybrid deep learning and machine learning models for crop yield prediction based on multitemporal satellite data. *Remote Sensing*, 14(4):861, 2022.
- [47] et al. Xu, Q. A gis-based probabilistic certainty factor approach for landslide susceptibility assessment in the zhongshan county, guangdong province, china. *Catena*, 140:113–125, 2016.
- [48] et al. Yuan, Z. Change detection meets foundation models: A comprehensive survey. *arXiv preprint arXiv:2402.12872*, 2024.
- [49] et al. Zhang, C. A deeply supervised image fusion network for change detection in remote sensing images. *ISPRS Journal of Photogrammetry and Remote Sensing*, 2020.
- [50] et al. Zhang, X. Aerial-cd: A large-scale aerial image change detection dataset and benchmark. *arXiv preprint arXiv:2306.05742*, 2023.
- [51] et al. Zhang, X. Changeclip: Remote sensing change detection with multimodal vision-language representation learning. *IEEE Transactions on Geoscience and Remote Sensing*, 2023.
- [52] et al. Zhao, Y. Detrs beat yolos on real-time object detection. In *Proceedings of the IEEE/CVF Conference on Computer Vision and Pattern Recognition (CVPR)*, page 10657220, 2024.
- [53] B. Zhou and P. Krähenbühl. Cross-view transformers for real-time map-view semantic segmentation. *Proceedings of the IEEE/CVF Conference on Computer Vision and Pattern Recognition*, pages 13760–13769, 2022.
- [54] Z. Zhu and C. E. Woodcock. Continuous change detection and classification of land cover using all available landsat data. *Remote Sensing of Environment*, 144:152–171, 2014.